



1 **Technical notes: rainfall threshold calculation for**
2 **debris flow early warning in areas with scarcity of**
3 **data**

4 **Hua-li Pan**^{1, 2}, **Yuan-jun Jiang**^{1, 2, ✉}, **Jun Wang**³, **Guo-qiang Ou**^{1, 2}

5 ✉ Corresponding author's e-mail: yuanjun.jiang.civil@gmail.com

6 ¹ Key Laboratory of Mountain Hazards and Earth Surface Process, Chinese Academy of Sciences, Chengdu
7 610041, China

8 ² Institute of Mountain Hazards and Environment, Chinese Academy of Sciences, Chengdu 610041, China

9 ³ Guangzhou Institute of Geography, Guangzhou 510070, China

10 **Abstract:** Debris flows are one of the natural disasters that frequently occur in mountain
11 areas, usually accompanied by serious loss of lives and properties. One of the most used ap-
12 proaches to mitigate the risk associated to debris flows is the implementation of early warning
13 systems based on well calibrated rainfall thresholds. However, many mountainous areas have
14 little data regarding rainfall and hazards, especially in debris flow forming regions. Therefore,
15 the traditional statistical analysis method that determines the empirical relationship between
16 rainfall and debris flow events cannot be effectively used to calculate reliable rainfall thre-
17 shold in these areas. To solve this problem, this paper developed a quantitative method to
18 identify rainfall threshold for debris flow early warning in data-poor areas based on the initia-
19 tion mechanism of hydraulic-driven debris flow. First, we studied the characteristics of the
20 study area, including meteorology, hydrology, topography and physical characteristics of the
21 loose solid materials. Then, the rainfall threshold was calculated by the initiation mechanism
22 of the hydraulic debris flow. The results show that the proposed rainfall threshold curve is a
23 function of the antecedent precipitation index and 1-h rainfall. The function is a line with a
24 negative slope. To test the proposed method, we selected the Guojuanyan gully, a typical de-
25bris flow valley that during the 2008-2013 period experienced several debris flow events and



26 that is located in the meizoseismal areas of Wenchuan earthquake, as a case study. We com-
27 pared the calculated threshold with observation data, showing that the accuracy of the method
28 is satisfying and thus can be used for debris flow early warning in areas with scarcity of data.

29 **Keywords:** Debris flow; rainfall threshold curve; rainfall threshold; areas with scarcity of
30 data

31 **1 Introduction**

32 Debris flow is rapid, gravity-induced mass movement consisting of a mixture of water,
33 sediment, wood and anthropogenic debris that propagate along channels incised on mountain
34 slopes and onto debris fans (Gregoretti et al., 2016). It has been reported in over 70 countries
35 in the world and often causes severe economic losses and human casualties, seriously
36 retarding social and economic development (Tecca and Genevois, 2009; Degetto et al., 2015;
37 Tiranti and Deangeli, 2015; McCoy et al., 2012; Imaizumi et al., 2006; Hu et al., 2016; Cui et
38 al., 2011; Dahal et al., 2009; Liu et al., 2010). On 12 May 2008, the Wenchuan earthquake
39 occurred in the Longmenshan tectonic belt on the eastern edge of the Tibetan plateau, China
40 (Xu et al., 2008; Wang and Meng, 2009). A huge amount of loose deposits remained in the
41 channels and on the slopes of the plateau after the Wenchuan earthquake. These loose
42 deposits have served as source materials for debris flow and shallow landslide in the years
43 since the earthquake (Tang et al. 2009, 2012; Xu et al. 2012; Hu et al. 2014). In the following
44 years since the earthquake, intense rainfall events have triggered massive debris flow that
45 have caused serious casualties and property loss, such as the Zhouqu debris flow and the
46 Wenjia gully debris flow which both occurred in 2010.

47 As an important and effective means of disaster mitigation, debris flow early warning
48 have received much attention from researchers. The rainfall threshold is the core of the early
49 warning of debris flow, a large number of scientists have made lots of researches yet (Chen
50 and Huang 2010; Cannon et al., 2008; Winter et al., 2013; Segoni et al., 2015; Staley et al.,
51 2013; Baum and Godt, 2010; Rosi et al 2015; Zhou and Tang, 2014). Although the formation
52 mechanism of debris flow has been extensively studied, it is difficult to perform distributed
53 physically based modeling over large areas, mainly because the spatial variability of
54 geotechnical parameters is very difficult to assess (Tofani et al., 2017). Therefore, many



55 researchers (Wilson and Joyko, 1997; Campbell, 1975; Cheng et al., 1998) have had to
56 determine the empirical relationship between rainfall and debris flow events and to determine
57 the rainfall threshold depending on the combinations of rainfall parameters, such as
58 antecedent rainfall, rainfall intensity, cumulative rainfall, etc. Cui (1991), Takahashi (1978)
59 and Iverson (1989) predicted the formation of debris flow based on studies of slope stability,
60 hydrodynamic action and the influence of pore water pressure on the formation process of
61 debris flow. Caine (1980) first statistically analyzed the empirical relationship between rainfall
62 intensity and the duration of debris flows and shallow landslides and proposed an exponential
63 expression ($I = 14.82D^{-0.39}$). Afterwards, other researchers, such as Wiczorek (1987), Jison
64 (1989), Hong et al. (2005), Dahal and Hasegawa (2008), Guzzetti et al. (2008) and Saito et al.
65 (2010), carried out further research on the empirical relationship between rainfall intensity
66 and the duration of debris flows, established the empirical expression of rainfall intensity -
67 duration ($I = D$) and proposed debris flow prediction models. Shiedand Chen (1995)
68 established the critical condition of debris flow based on the relationship between cumulative
69 rainfall and rainfall intensity. Zhang (2014) developed a model for debris flow forecasting
70 based on the water-soil coupling mechanism at the watershed scale. Tang et al. (2012)
71 analyzed the critical rainfall of Beichuan city and found that the cumulative rainfall
72 triggering debris flow decreased by 14.8%-22.1% when compared with the pre-earthquake
73 period, and the critical hour rainfall decreased by 25.4%-31.6%. Chen et al. (2013) analyzed
74 the pre- and post-earthquake critical rainfall for debris flow of Xiaogangjian gully and found
75 that the critical rainfall for debris flow in 2011 was approximately 23% lower than the value
76 during the pre-earthquake period. Other researches, such as Chen et al. (2008) and Shied et al.
77 (2009) has reached similar conclusions that the post-earthquake critical rainfall for debris
78 flow is markedly lower than that of the pre-earthquake period. Zhenlei Wei et al. (2017)
79 investigated a rainfall threshold method for predicting the initiation of channelized debris
80 flows in a small catchment, using field measurements of rainfall and runoff data.

81 Overall, the studies on the rainfall threshold of debris flow can be summarized as two
82 methods: the demonstration method and the frequency calculated method. The
83 demonstration method employs statistical analysis of rainfall and debris flow data to study the
84 relationship between rainfall and debris flow events and to obtain the rainfall threshold curve



85 (Bai et al., 2008; Zhuang, et al., 2009; Tian et al., 2008). This method is relatively accurate,
86 but it needs very rich, long-term rainfall sequence data and disaster information; therefore, it
87 can be applied only to areas with a history of long-term observations, such as Jiangjiagou,
88 Yunnan, China, and Yakedake, Japan. The frequency calculated method, based on the
89 assumption that debris flow and torrential rain have the same frequency, and thus, a debris
90 flow rainfall threshold can be calculated based on the rainstorm frequency in the mountain
91 towns that have abundant rainfall data but lack of disaster data (Yao, 1988; Liang and Yao,
92 2008). Researchers have also analyzed the relationship between debris flow occurrences and
93 precipitation and soil moisture content based on initial debris flow conditions (Hu and Wang,
94 2003). However, this approach is rarely applied to the determination of debris flow rainfall
95 thresholds. Pan et al. (2013) calculated the threshold rainfall for debris flow pre-warning by
96 calculating the critical depth of debris flow initiation combined with the amount and
97 regulating factors of runoff generation.

98 Most mountainous areas have little data regarding rainfall and hazards, especially in
99 Western China. When a debris flow outbreak occurs, it often causes serious harm to villages,
100 farmland, transport centers and water conservation facilities in the downstream area. Neither
101 the traditional demonstration method nor frequency calculated method can satisfy the debris
102 flow early warning requirements in these areas. Therefore, how to calculate the rainfall
103 threshold in these data-poor areas has become one of the most important challenges for the
104 debris flow early warning systems. To solve this problem, this paper developed a quantitative
105 method of calculating rainfall threshold for debris flow early warning in data-poor areas based
106 on the initiation mechanism of hydraulic-driven debris flows.

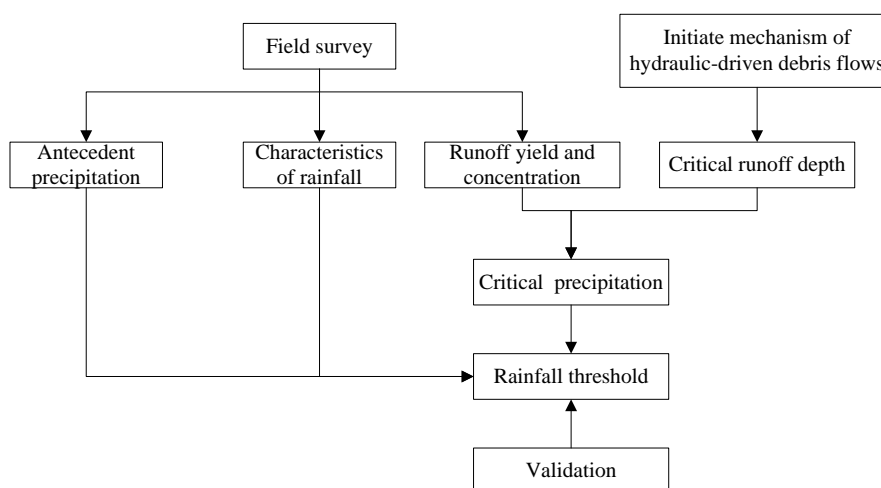
107 **2 Materials and methods**

108 This study makes an attempt to analyze the trigger rainfall threshold for debris flow
109 by using the initiation mechanism of debris flow. The characteristics of rainfall in the wa-
110 tershed were analyzed firstly by the field survey. At the same time, the critical runoff
111 depth to initiate debris flow was calculated by the initiation mechanism with the under-
112 lying surface condition (materials, longitudinal slope, etc.) of the gully. Then, the corres-
113 ponding rainfall for the initiation of debris was back-calculated based on the hypothesis



114 that runoff generation under saturated condition. At last, these factors were combined to
115 build the rainfall threshold model. This method can be applied to the early warning sys-
116 tem in the areas with scarcity of rainfall data.

117 The flow chart of the research is shown in Figure 1.



118

119

Figure 1 The flow chart of the research

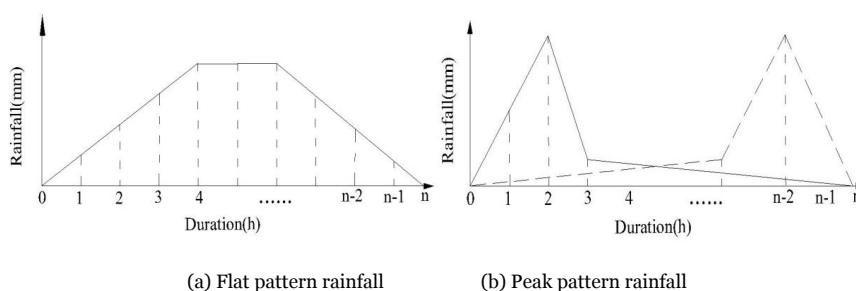
120 **2.1 Rainfall pattern and the spatial-temporal distribution characteristics**

121 Mountain hazards such as debris flows are closely related to rainfall duration, rain-
122 fall amount and rainfall pattern (Liu et al., 2009). Rainfall pattern not only affects the
123 formation of surface runoff but also affects the formation and development of debris
124 flows. Different rainfall patterns result in different soil water contents; thus, the internal
125 structure of the soil, stress conditions, corrosion resistance, slip resistance and removable
126 thickness can vary. The initiation of a debris flow is the result of both short-duration
127 heavy rains and the antecedent rainfall. Many previous observational data have shown
128 that the initiation of a debris flow often appears at a certain time that has a high correla-
129 tion with the rainfall pattern (Guido Rianna, 2014; Mohamad Ayob Mohamadi, 2015).

130 Based on the rainfall characteristics, rainfall patterns can be roughly divided into two
131 kinds, the flat pattern and the peak pattern, as shown in Figure 2. If the rainfall intensity
132 has little variation, there is no obvious peak in the whole rainfall process; such rainfall



133 can be described as flat pattern rainfall. And the debris flows, if occur, are mainly caused
 134 by the great amount of antecedent precipitation. While if the rainfall intensity increases
 135 suddenly during a certain period of time, the rainfall process will have an obvious peak
 136 and is termed peak pattern rainfall. And these debris flows are mainly controlled by the
 137 short-duration heavy rains. Peak pattern rainfall may have one peak or more than one
 138 peak (Pan, et al., 2013).

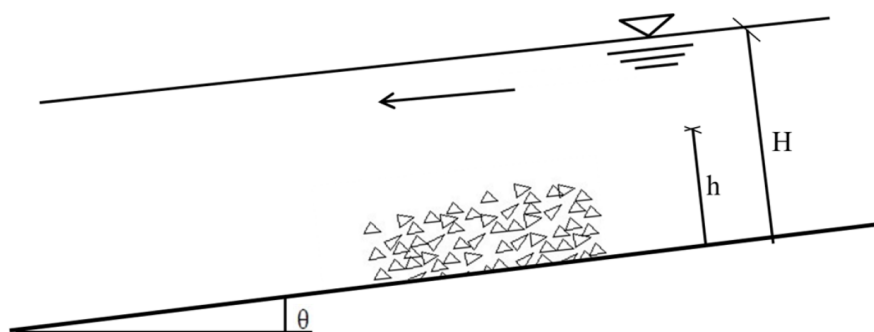


141 **Figure 2** The diagram of rainfall patterns

142 Through analyzing the rainfall data of the Guojuanyan gully, the rainfall pattern and
 143 the spatial-temporal distribution characteristics can be obtained.

144 **2.2 The rainfall threshold curve of debris flows**

145 **2.2.1 The initiation mechanism of hydraulic-driven debris flows**



148 **Figure 3** The typical debris flow initiate model

148 When the watershed hydrodynamics, which include the runoff, soil moisture content



149 and the discharge, reach to a certain level, the loose deposits in the channel bed will in-
 150 itiate movement and the sediment concentration of the flow will increase, leading the se-
 151 diment laden flow to transform into a debris flow. The formation of this kind of debris
 152 flow is a completely hydrodynamic process.

153 Figure 3 shows a simple hydraulic-driven debris flow initiate model, where h is the
 154 probable erosion depth (m), H is the whole depth from gully surface to the bottom (m),
 155 and θ is the longitudinal slope of gully ($^{\circ}$). Takahashi (1977) established a model for
 156 the initiation of hydraulic-driven debris flow, which can be expressed as follows:

$$157 \quad S_v = \frac{\gamma \tan \theta}{(\gamma_s - \gamma)(\tan \alpha - \tan \theta)} \quad (1)$$

$$158 \quad \tan \theta \geq \frac{S'_{vm}(\gamma_s - \gamma) \tan \phi}{S'_{vm}(\gamma_s - \gamma) + \gamma(H/h)} \quad (2)$$

159 In these formulas, S_v is the volume concentration of sediment, S'_{vm} is the average
 160 volume concentration of stratification flow, γ is the density of water (g/cm^3), γ_s is the
 161 density of solids (g/cm^3), and $\tan \phi$ is the macroscopic friction coefficient among the
 162 particles, θ is the longitudinal slope of gully ($^{\circ}$).

163 The Takahashi's model became one of the most common for the initiation of debris
 164 flow. Several related studies were published based on Takahashi's model later. Some dis-
 165 cussed the laws of debris flow according to the geomorphology and the water content
 166 while others examined the critical conditions of debris flow with mechanical stability
 167 analysis.

168 This study aims to the initiation of loose solid materials in the gully; therefore, it can
 169 be regarded as the initiation problem of debris flow under hydrodynamic force. According
 170 to Takahashi's model, the critical depth for hydraulic-driven debris flows is:

$$171 \quad h_0 = \left[\frac{C_s(\sigma - \rho) \tan \phi}{\rho \tan \theta} - \frac{C_s(\sigma - \rho)}{\rho} - 1 \right] d_m \quad (3)$$

172 where C_s is the volume concentration obtained by experiments(0.812); σ is the density of
 173 loose deposits (usually is $2.65 \text{ t}/\text{m}^3$); ρ is the water density, $1.0 \text{ t}/\text{m}^3$, θ is the channel bed
 174 slope, ($^{\circ}$); ϕ is the internal friction angle ($^{\circ}$) and can be measured by shear tests ;



175 and d_m is the average grain diameter (mm), which can be expressed as:

176
$$d_m = \frac{d_{16} + d_{50} + d_{84}}{3} \quad (4)$$

177 where d_{16} , d_{50} and d_{84} are characteristic particle sizes of the loose deposits (mm).

178 **2.2.2 Calculation of watershed runoff yield and concentration**

179 The Guojuanyan gully is located in Du Jiangyan city, which is in a humid area.
180 Therefore, stored-full runoff is the main pattern runoff yield in this gully, and this runoff
181 yield pattern is used to calculate the watershed runoff. That is, it is supposed that the wa-
182 ter storage can reach the maximum storage capacity of the watershed after each heavy
183 rain. Therefore, the rainfall loss in each time I is the difference between the maximum
184 water storage capacity I_m and the soil moisture content before the rain P_a . Hence, the wa-
185 ter balance equation of stored-full runoff is expressed as follows (Ye, et al., 1992):

186
$$R = P - I = P - (I_m - P_a) \quad (5)$$

187 where R is the runoff depth (mm); P is the precipitation of one rainfall (mm); I is the
188 rainfall loss (mm); I_m is the watershed maximum storage capacity (mm) for a certain
189 watershed, it is a constant for a certain watershed that can be calculated by the infiltra-
190 tion curve or infiltration experiment data. In this study, I_m has been picked up from
191 Handbook of rainstorm and flood in Sichuan (Sichuan Water and Power Department
192 1984); and P_a is the antecedent precipitation index, referring to the total rainfall prior to
193 the 1 hour peak rainfall leading to debris flow initiation.

194 Eq. 5 can be expressed as follows:

195
$$P + P_a = R + I_m \quad (6)$$

196 In this study, P and P_a are replaced by I_{60} (1 hour rainfall) and API (the antecedent
197 precipitation index), respectively; thus, Eq. 6 is expressed as:

198
$$I_{60} + API = R + I_m \quad (7)$$

199 In the hydrological study, the runoff depth R is:



$$R = \frac{W}{1000F} = \frac{3.6 \sum Q \cdot \Delta t}{F} = \frac{3.6Q}{F} \quad (8)$$

201 where R is the runoff depth (m); W is the total volume of runoff (m^3); F is the watershed
202 area (km^2); Δt is the computational time step; and Q is the average flow of the watershed
203 (m^3/s), which can be expressed as follows:

$$Q = BVh_0 \quad (9)$$

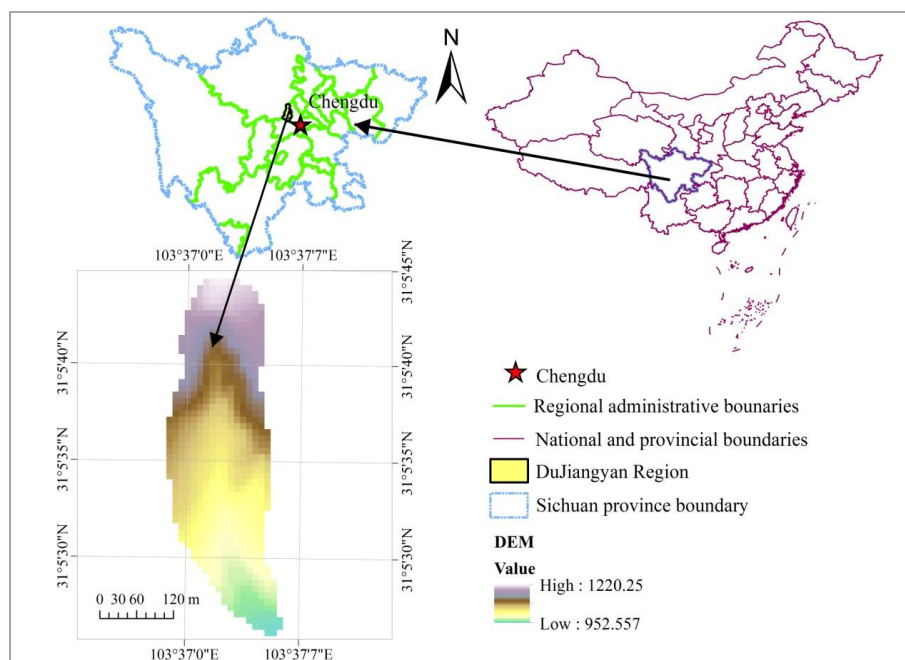
205 where B is the width of the channel (m), V is the average velocity (m/s) and h_0 is the critical
206 depth (m).

207 Eq. 7 is the expression of the rainfall threshold curve for a watershed, which can be
208 used for debris flow early warning. This proposed rainfall threshold curve is a function of
209 the antecedent precipitation index (API) and 1 hour rainfall (I_{60}), which is a line and a
210 negative slope.

211 3 Case study

212 3.1 Location and gully characteristics of the study area

213 The Guojuanyan gully in Du Jiangyan city, located in the meizoseismal areas of the
214 Wenchuan earthquake, China, was selected as the study area (Figure 4). It is located at
215 the Baisha River, which is the first tributary of the Minjiang River. The seismic intensity
216 of the study area was XI, which was the maximum seismic intensity of the Wenchuan
217 earthquake. The Shenxi Gully Earthquake Site Park is at the right side of this gully. The
218 area extends from $31^{\circ}05'27''$ N to $31^{\circ}05'46''$ N latitude and $103^{\circ}36'58''$ E to $103^{\circ}37'09''$
219 E longitude, covering an area of 0.15 km^2 with a population of 20 inhabitants. The
220 elevation range is from 943 m to 1222 m, the average gradient of the main channel is
221 270‰, and the length of the main channel is approximately 580m.



222

223

Figure 4 The location of the Guojuanyan gully

224

Geologically, the Guojuanyan gully is composed of bedrock and Quaternary strata.

225

The bedrock is upper Triassic Xujiahe petrofabric (T_{3x}) whose lithology is mainly

226

sandstone; mudstone; carbonaceous shale belonging to layered, massive structures; and

227

semi solid-solid petrofabric. The Quaternary strata are alluvium (Q_4^{el+pl}), alluvial

228

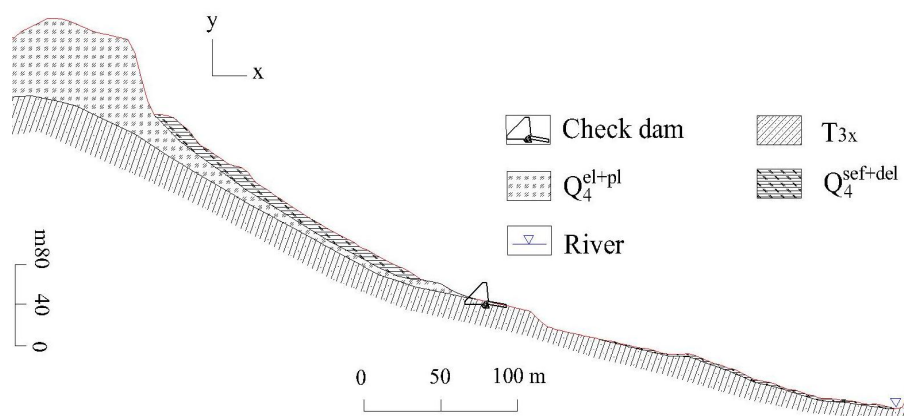
materials (Q_4^{pl+dl}), landslide accumulations and debris flow deposits ($Q_4^{sef+del}$). The

229

thickness of the Quaternary strata ranges from 1 m to 20 m and varies greatly. The strata

230

profile of the Guojuanyan gully is shown in Figure 5.



231

232

Figure 5 The strata profile of the Guojuanyan gully (Jun Wang et al, 2017)

233

234

235

236

237

238

239

240

Geomorphologically, the study area belongs to the Longmenshan Mountains. The famous Longmenshan tectonic belt has a significant effect on this region, especially the Hongkou- Yinxu fault. The study area has strong tectonic movement and strong erosion, and the main channel is “V”-shaped. The area is characterized by a rugged topography, and the main slope gradient interval of the gully is 20° to 40° , accounting for 52.38% of the entire study area.

Climatically, this area has a subtropical and humid climate, with an average annual temperature of 15.2°C and an average annual rainfall of 1200 mm (Wang et al., 2014).

241

3.2 Materials and debris flow characteristics of the study area

242

243

244

245

246

247

248

249

The Wenchuan earthquake generated a landslide in the Guojuanyan gully, leading to an abundance of loose deposits that have served as the source materials for debris flows. A comparison of the Guojuanyan gully before and after the Wenchuan earthquake is shown in Figure 6. The field investigations show that the volume of materials is more than $20 \times 10^4 \text{ m}^3$. Therefore, the trigger rainfall for debris flow has decreased greatly. The Guojuanyan gully had no debris flows before the earthquake; however, it became a debris flow gully after the earthquake, and debris flows occurred in the following years (Table 1). The field investigations and experiments determined that the density of the debris flow



250 was between 1.8 and 2.1 g/cm³.



251

252

(a) 14 September, 2006 (b) 28 June, 2008

253 **Figure 6** The Guojuanyan gully before (a) and after the Wenchuan earthquake (b) (from Google Earth)

254 **Table 1** The frequency table of debris flow pre- and post-Wenchuan earthquake in the study area

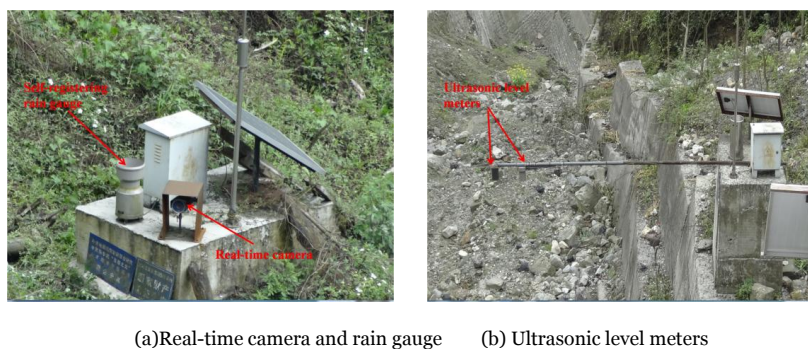
Before the earthquake		After the earthquake							
Before 2008	2008	2009	2010	2011	2012	2013	2014		
No record	24 September	17 July	13 August	17 August	1 July	17 August	9 July	26 July	18 July

255 3.3 Debris flow monitoring and streambed survey of the study area

256 After the Wenchuan earthquake, continuous field surveillance was undertaken in the
 257 study area. A debris flow monitoring system was also established in the study area. To
 258 identify the debris flow events, this monitoring system recorded stream water depth, pre-
 259 cipitation and real-time video of the gully (Figure 7). The water depth was measured us-
 260 ing an ultrasonic level meter, and precipitation was recorded by a self-registering rain
 261 gauge. The real-time video was recorded onto a data logger and transmitted to the moni-
 262 toring center, located in the Institute of Mountain Hazards and Environment, Chinese
 263 Academy of Sciences. When an abnormal rainfall or a debris flow event occurs, the real-
 264 time data, including rainfall data, video record, and water depth data, can be observed
 265 and queried directly in the remote client computer in the monitoring center. Figure 8
 266 shows images taken from the recorded video. These data can be used to analyze the rain-
 267 fall or other characteristics, such as the 10-min, 1- and 24-h critical rainfall. The recorded



268 video is usually used to analyse the whole inundated process of debris flow events and to
269 identify debris flow events as well as the data from rainfall, flow depth, and field investi-
270 gation.



271
272
273

Figure 7 Debris flow monitoring system in the study area



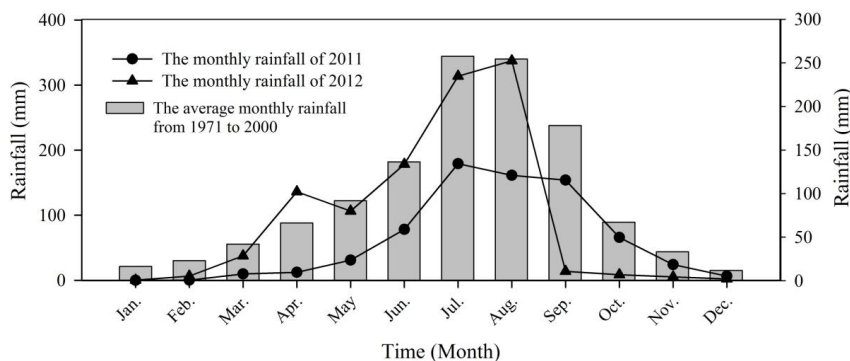
274
275

Figure 8 Real-time images from video taken during the debris flow movement

276 3.4 Data collection and the characteristics of rainfall

277 The Wenchuan earthquake occurred in the Longmenshan tectonic belt, located on
278 the eastern edge of the Tibetan plateau, China, which is one of three rainstorm areas of
279 Sichuan Province (Longmen mountain rainstorm area, Qingyi river rainstorm area and
280 Daba mountain rainstorm area). Heavy rainstorms and extreme rainfall events occur fre-
281 quently. The spatial-temporal variability of rainfall has the following characteristics:

282 (1) Abundant precipitation: The average annual precipitation was 1177.3 mm from
283 1971 to 2000, and the average monthly precipitation is shown in Figure 10. From 1971 to
284 2000, the minimum annual precipitation of 713.5 mm occurred in 1974, and the maxi-
285 mum annual precipitation of 1605.4 mm occurred in 1978.



286

287 **Figure 9** The average monthly precipitation of the Guojuanyan gully from 1971 to 2000 and the
288 monthly rainfall of 2011 and 2012

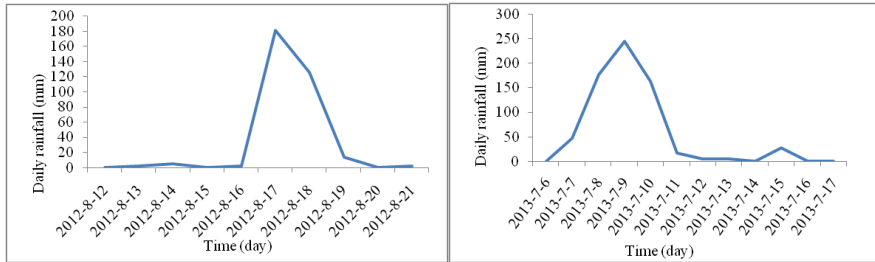
289 (2) Severely inhomogeneous distribution of precipitation in time: from Figure 9 we
290 can observe that rainfall is seasonal, with approximately 80% of the total rainfall occur-
291 ring during the monsoon season (from June to September) and the other 20% in other
292 seasons. For instance, in 2012, the total annual rainfall in this area was approximately
293 1148 mm, and rainfall in the monsoon season from June to September was 961 mm, ac-
294 counting for 83.7% of the annual total.

295 (3) Due to the impact of the atmospheric environment, the regional and annual dis-
296 tribution of rainfall is seriously inhomogeneous; moreover, the rainfall intensity has great
297 differences. From 1957 to 2008, the maximum monthly rainfall was 592.9 mm, the daily
298 maximum rainfall was 233.8 mm, the hourly maximum rainfall was 83.9 mm, the 10
299 minute maximum rainfall was 28.3 mm, and the longest continuous rainfall time was 28
300 days.

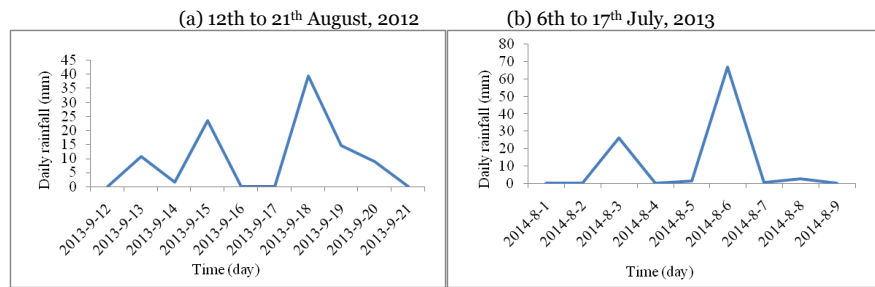
301 Debris flow field monitoring data and on-site investigation data were used to identify
302 the debris flow events and to analyze the characteristics of the rainfall pattern and the
303 critical rainfall characteristics. From several typical rainfall process curves (Figure 10),
304 the rainfall pattern of the Guo Juanyan gully is the peak pattern, displaying the single
305 peak and multippeak, a characteristic of short-duration rainstorms. Through the statistical
306 analysis of the 10-min, 1-, and 24-h critical rainfall of debris flow events after the earth-
307 quake, their characteristics can be obtained, as shown in Figure 11.



308



309



310

311

312

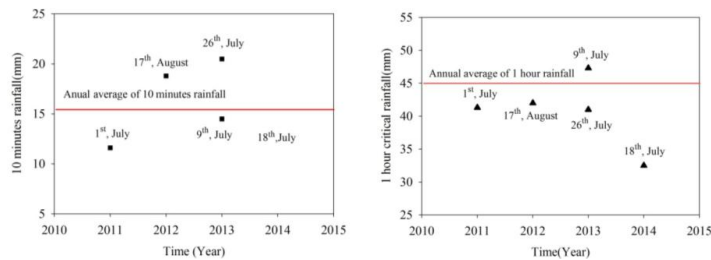
(c) 12th to 21th September, 2013

(d) 1st to 9th August, 2014

Figure 10 The typical rainfall process curves of the Guojuanyan gully

313

314



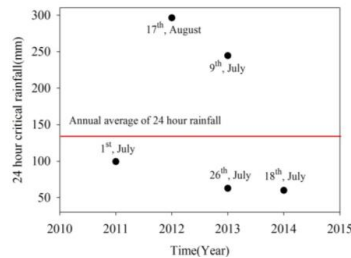
(a) The 10-min critical rainfall

(b) The 1-h critical rainfall

315

316

317



(c) The 24-h critical rainfall

Figure 11 The critical rainfall of debris flows in the Guojuanyan gully



318 Figure 11a shows that the observed 10-min critical rainfall is between 11.1 mm and
319 21.5 mm. According to the Sichuan Hydrology Record Handbook (Sichuan Water and
320 Power Department 1984), the annual average 10-min rainfall of the study area is ap-
321 proximately 15.1 mm. According to the observation, 60% of debris flow events occurred
322 below the annual average 10-min rainfall. In addition, the 1-h critical rainfall varied be-
323 tween 34.5 mm and 47.3 mm in the study area (Figure 11b). And the annual average 1-h
324 rainfall is 45.0 mm based on the Sichuan Hydrology Record Handbook (Sichuan Water
325 and Power Department 1984). Figure 11b shows that 80% debris flow events occurred
326 below the annual average 1-h rainfall, except for the debris flow event occurred on July 9,
327 2013. At last, the minimum value of 24-h critical rainfall is 60.4 mm and the maximum
328 value is 296.4 mm in the study area. According to the Sichuan Hydrology Record Hand-
329 book (Sichuan Water and Power Department 1984), the annual average 24-h rainfall is
330 132 mm. From Figure 11c, we can see that 24-h critical rainfall for different debris flow
331 events vary widely and 60% debris flow events occurred below the annual average 24-h
332 rainfall.

333 From the above study, we can find that the 10-min and the 1-h critical rainfalls of
334 different debris flow events have minor differences; however, the 24-h critical rainfalls
335 vary widely. The reason is that debris flow is usually triggered by short-duration rains-
336 torms. Therefore, the short-durations of 10-min and 1-h rainfall have higher correlation
337 with debris flow occurrence and have the minor differences. Further analyzing the 10-min
338 and 1-h critical rainfalls, we can find that they vary with the antecedent precipitation in-
339 dex (API). They are variable rather than constant. In this paper, the antecedent precipi-
340 tation index (API) and the 1-h rainfall (I_{60}) were used to calculate the rainfall threshold
341 curve of debris flows in the Guojuanyan gully.

342 The 10-min, 1-h and 24-h rainfalls changed little pre- and post-Wenchuan earth-
343 quake, but the debris flow activity differ considerably. The Guo Juanyan gully has no de-
344bris flows under the annual average rainfall before 2008, but it became a debris flow gully
345 after the earthquake under the same conditions, even the rainfall was smaller than the
346 annual average rainfall. This indicates that earthquakes have a big influence on debris



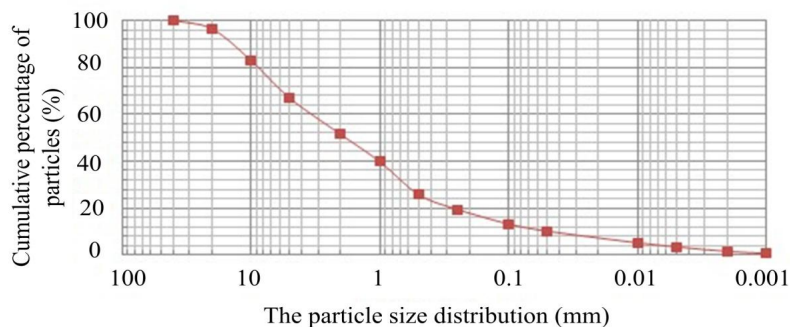
347 flow occurrence. The Wenchuan earthquake triggered a landslide in the Guo Juanyan
 348 gully and a huge volume of loose deposits was present on the channels and slopes. These
 349 loose deposits provide abundant loose source materials for debris flow activity. Therefore,
 350 the rainfall threshold of debris flow post-earthquake is an important and urgent issue to
 351 study for debris flow early warning and mitigation.

352 4 Results

353 4.1 The rainfall threshold curve of debris flow

354 4.1.1 The critical depth of the Guojuanyan gully

355 The grain grading graph (Figure 12) is obtained by laboratory grain size analysis ex-
 356 periments for the loose deposits of the Guojuanyan gully. Figure 13 shows that the cha-
 357 racteristic particle sizes d_{16} , d_{50} , d_{84} and d_m are 0.18 mm, 1.9 mm, and 10.2 mm, 4.1 mm,
 358 respectively. According to Eq. (1), the critical depth (h_0) of the Guojuanyan gully is 7.04 mm.



359
 360 **Figure 12** The grain grading graph of the Guojuanyan gully

361 **Table 2** Critical water depth of debris flow triggering in Guojuanyan gully

C_s	σ (g/cm ³)	ρ (g/cm ³)	$\tan \theta$	d_{16} (mm)	d_{50} (mm)	d_{84} (mm)	d_m (mm)	ϕ (°)	$\tan \phi$	h_0 (mm)
0.812	2.67	1.0	0.333	0.18	1.9	10.2	4.1	21.21	0.388	7.04

362 4.1.2 The rainfall threshold curve of debris flow

363 Taking the cross-section at the outlet of the debris flow formation region as the



364 computation object, based on the field investigations and measurements, the width of the
 365 cross-section is 20 m, and the average velocity of debris flows is 1.5m/s. Based on the
 366 Handbook of rainstorm and flood in Sichuan (Sichuan Water and Power Department
 367 1984), the watershed maximum storage capacity (I_m) of the Guojuanyan gully is 100mm.
 368 The calculated rainfall threshold curve of debris flow in the Guojuanyan gully is shown in
 369 Table 3.

370 **Table 3** The calculated process of the rainfall threshold

Watershed	h_0 (mm)	B (m)	V (m/s)	Q (m ³ /s)	Δt (h)	F (km ²)	R (mm)	I_m (mm)	$R + I_m$ (mm)
Guojuanyan	7.04	20.0	1.5	0.197	1	0.11	6.9	100	106.9

371 From the calculated results, we can conclude the rainfall threshold of the debris flow
 372 is $I_{60} + API = R + I_m = 106.9 \approx 107$ mm; that is, when the sum of the antecedent precipita-
 373 tion index (API) and the 1 hour rainfall (I_{60}) reaches 107 mm (early warning area), the
 374 gully may trigger debris flow.

375 4.2 Validation of the results

376 4.2.1 The calculation of the antecedent precipitation index (API)

377 The 1 hour rainfall (I_{60}) is obtained from the observed data of the Guojuanyan gully.
 378 The antecedent precipitation index (API) is calculated as the following expression (Guo,
 379 2013; Zhuang, 2015; Zhao, 2011):

$$380 \quad API = P_{a0} + R, \quad (10)$$

381 where P_{a0} is the antecedent effective rainfall (mm) and R is the stimulating rainfall (mm),
 382 which can be expressed as:

$$383 \quad R_t = \sum_{t_0}^{t_n} r \quad (11)$$

384 where t_0 is the start time (days) for the rainfall on a given day, t_n is the time prior to the 1
 385 hour rainfall peak and r is the precipitation (mm).



386 The antecedent effective rainfall P_{a0} is:

$$387 \quad P_{a0} = KP_1 + K^2P_2 + K^3P_3 + \dots + K^n P_n \quad (12)$$

388 where P_n ($n=1, 2, 3, \dots, n$) is the daily rainfall prior to debris flow events (mm), and K is
 389 the decreasing coefficient ($K=0.8-0.9$), which is determined by weather conditions, such
 390 as sunny or cloudy conditions.

391 Eq.12 can be used to estimate the amount of solid material and the moisture content
 392 prior to the debris flow. The effect of a rainfall event usually diminishes within 20 days
 393 and decreases with lower daily K values. Different patterns of storm debris flow gullies
 394 require different numbers of previous indirect rainfall days, which can be determined by
 395 the relationship between the stimulating rainfall and the antecedent rainfall of a debris
 396 flow (Pan, et al., 2013). Generally, a typical rainstorm debris flow gully requires 20 days
 397 of antecedent rainfall.

398 In this paper, $n=20$ and $K=0.8$. The complete rainfall processes of debris flow
 399 events obtained from the observed data can be used to calculate P_{a0} , R_t , and API .

400 **4.2.2 The rainstorm and debris flow events in the Guojuanyan gully during**
 401 **2010-2014**

402 Table 1 shows that debris flows occurred almost every year after the earthquake. The con-
 403 ditions of the debris flow events were collected through field investigations and inter-
 404 views. The specific conditions of these debris flows are listed in Table 3. Unfortunately,
 405 there were no rainfall data before 2011, when we started field surveys in the Guojuanyan
 406 gully.

407 **Table 4** The specific conditions of debris flow events in the Guojuanyan gully after the earthquake

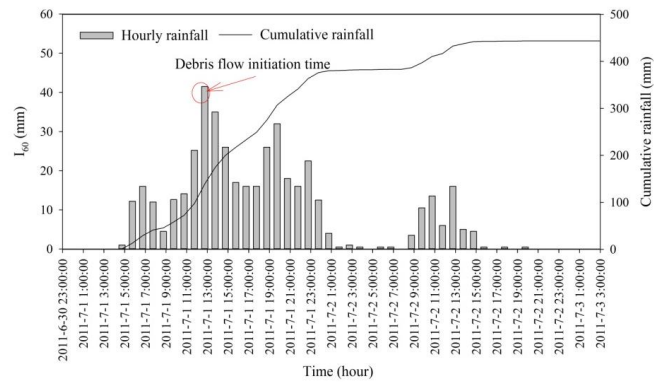
Time	Volume (10^4 m ³)	Surges	Rainfall data record
24 September, 2008	0.6	1	No
17 July, 2009	0.8	1	No
13 August, 2010	4.0	3	No
17 August, 2010	0.4	1	No
1 July, 2011	0.8	1	Yes
17 August, 2012	0.7	1	Yes
9 July, 2013	0.4	1	Yes
26 July, 2013	2.0	2	Yes



18 July, 2014 1.5 1 Yes

408

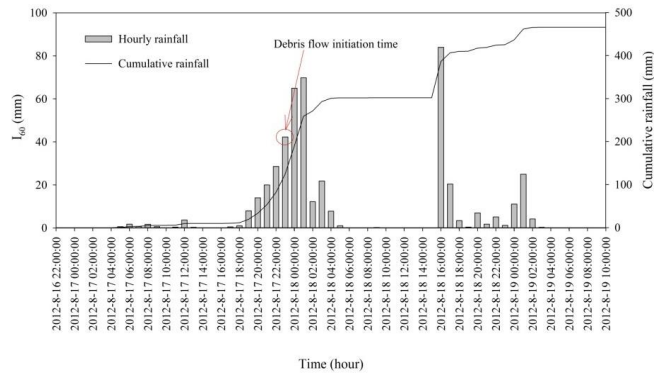
409 This study analyzed the rainfall process of the 5 debris flows (Figure 13) and calcu-
 410 lated the corresponding antecedent effective rainfall (P_{a0}), stimulating rainfall (R), and
 411 1 hour rainfall (I_{60}) (Table 5).



412

413

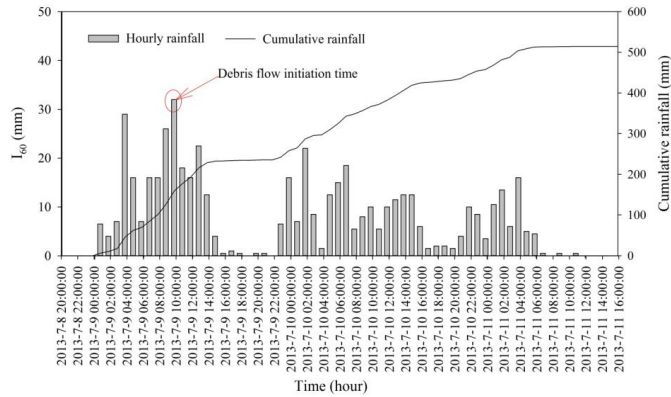
(a)



414

415

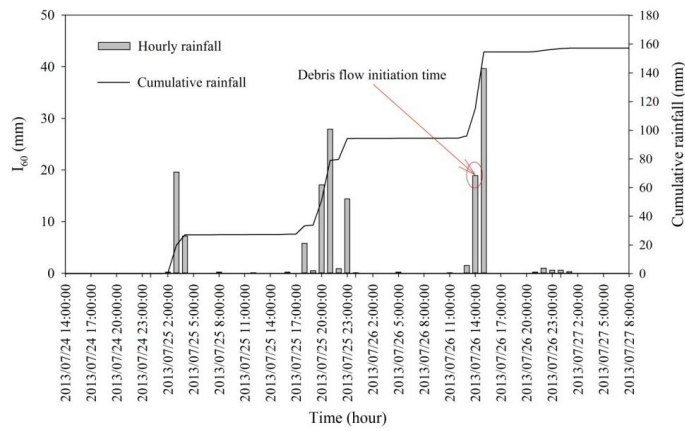
(b)



416

417

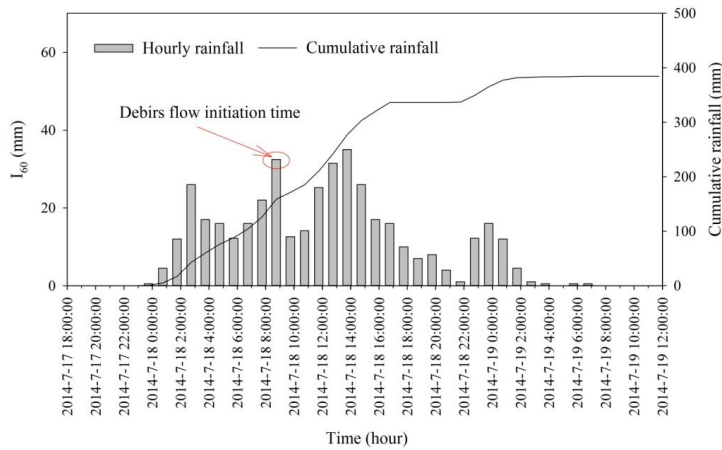
(c)



418

419

(d)



420

421

(e)



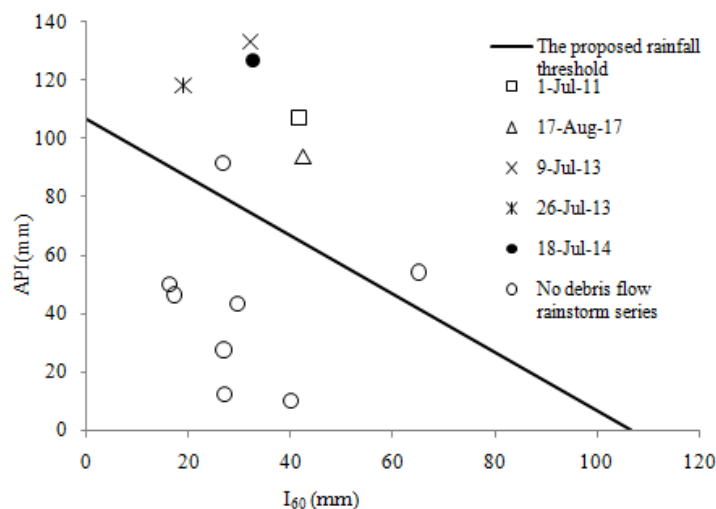
422

423 **Figure 13** The rainfall process of debris flow vents in the Guojuanyan gully from 2011 to 2014 (a, July 1,
 424 2011; b, August 17, 2012; c, July 9, 2013; d, July 26, 2013; e, July 18, 2014)

425 Furthermore, some typical rainfall whose daily rainfall was greater than 50 mm but
 426 did not trigger a debris flow were also calculated; the greatest 1-h rainfall is considered
 427 as I_{60} (Table 5).

428 **Table 5** The data of typical rainfall in the Guojuanyan gully after the earthquake

Time	Daily rainfall (mm)	Pa_0 (mm)	R_t (mm)	API (mm)	I_{60} (mm)	$API+I_{60}$ (mm)	Location to the threshold line	Trigger debris flow
1 July, 2011		9.7	97.6	107.3	41.5	148.8	Above	Yes
17 August, 2012		12.1	81.9	94.0	42.3	136.3	Above	Yes
9 July, 2013		5.7	127.5	133.2	32	165.2	Above	Yes
26 July, 2013		22.4	96.0	118.4	18.9	137.3	Above	Yes
18 July, 2014		10.7	116.2	126.9	32.5	159.4	Above	Yes
20 August, 2011	82.8	8.5	19.0	27.5	26.8	54.3	Below	No
5 September, 2011	52.1	48.7	1.2	49.9	16.2	66.1	Below	No
16 June, 2012	55.8	5.6	6.6	12.2	27.0	39.2	Below	No
3 August, 2012	148.3	7.5	84.3	91.8	26.7	118.5	Above	No
18 August, 2012	125.7	54.3	0	54.3	65.0	119.3	Above	No
18 June, 2013	50.6	6.2	3.8	10.0	40.0	50.0	Below	No
28 July, 2013	59.4	13.4	30.0	43.4	29.4	72.8	Below	No
6 August, 2013	56.1	12.4	34.0	46.4	17.1	63.5	Below	No



429

430 **Figure 14** The proposed rainfall threshold curve of debris flow in the Guojuanyan gully

431



432 The proposed rainfall threshold curve is a function of the antecedent precipitation
433 index (API) and 1-h rainfall (I_{60}), which is a line and a negative slope. Figure 14 shows
434 that the calculated values $I_{60} + API$ of debris flow events in the Guojuanyan gully are all
435 above the rainfall threshold curve, while most of the rainstorms that did not trigger debris
436 flow were below the curve. That is, the proposed rainfall threshold curve is reasonable
437 through the validation by rainfall and hazards data of the Guojuanyan gully.

438 **5 Discussions**

439 The proposed rainfall threshold curve is a function of the antecedent precipitation
440 index (API) and the 1-h rainfall (I_{60}), which has been validated by rainfall and hazards
441 data and can be applied to debris flow early warning and mitigation. However, the special
442 prone environment of debris flow after earthquake caused the rainfall threshold is much
443 more complex and uncertain. The rainfall threshold of debris flows varies with the ante-
444 cedent precipitation index (API), rainfall characteristics, amount of loose deposits,
445 channel and slope characteristics, and so on. In Figure 14, there are two points above the
446 curve that did not trigger debris flow at all; therefore, we should further study the cha-
447 racteristics of the movable solid materials and other factors.

448 In addition, restricted by the limited rainfall data, this study was validated by only 5
449 debris flow events. The value of the curve should be further validated and continuously
450 corrected with more rainfall and disaster data in later years.

451 The proposed approach in this study is based on the physical process of debris flow
452 initiation. As the initiation depth in distinct watershed is different from each other be-
453 cause of the different topography and loose solid materials, hence the rainfall threshold is
454 independent for each watershed. While most of debris flow gullies in Wenchuan earth-
455 quake affected areas with scarcity of rainfall data and disaster data, therefore, the ap-
456 proach presented in this study hasn't been validated by other gullies except the Guojua-
457 nyan gully so far.

458 **6 Conclusions**



459 (1) In the Wenchuan earthquake-stricken areas, loose deposits are widely distri-
460 buted, causing dramatic changes on the environmental development for the occurrence of
461 debris flow; thus, the debris flow occurrence increased dramatically in the subsequent
462 years. The characteristics of the 10-min, 1-h and 24-h critical rainfalls were represented
463 based on a comprehensive analysis of limited rainfall and hazards data. The statistical
464 results show that the 10-min and 1-h critical rainfalls of different debris flow events have
465 minor differences; however, the 24 hour critical rainfalls vary widely. The 10-min and 1-h
466 critical rainfalls have a notably higher correlation with debris flow occurrences than to
467 the 24-h critical rainfalls.

468 (2) The rainfall pattern of the Guojuanyan gully is the peak pattern, both single peak
469 and multi-peak. The antecedent precipitation index (*API*) was fully explored by the an-
470 tecedent effective rainfall and stimulating rainfall.

471 (3) As an important and effective means of debris flow early warning and mitigation,
472 the rainfall threshold of debris flow was determined in this paper, and a new method to
473 calculate the rainfall threshold is put forward. Firstly, the rainfall characteristics, hydro-
474 logical characteristics, and some other topography conditions were analysed. Then, the
475 critical water depth for the initiation of debris flows is calculated according to the topo-
476 graphy conditions and physical characteristics of the loose solid materials. Finally, ac-
477 cording to the initiation mechanism of hydraulic-driven debris flow, combined with the
478 runoff yield and concentration laws of the watershed, this study promoted a new method
479 to calculate the debris flow rainfall threshold. At last, the hydrological condition for the
480 initiation of a debris flow is the result of both short-duration heavy rains (I_{60}) and the
481 antecedent precipitation index (*API*). The proposed approach resolves the problem of
482 debris flow early warning in areas with scarcity data, can be used to establish warning
483 systems of debris flows for similar catchments in areas with scarcity data. This study pro-
484 vides a new thinking for the debris flow early warning in the mountain areas.

485 **Acknowledgments**



486 This paper is supported by the CRSRI Open Research Program (Program SN:
487 CKWV2015229/KY), CAS Pioneer Hundred Talents Program, and National Nature Science
488 Foundation of China (No. 41372331 & No. 41672318).

489 **References**

- 490 Bai LP, Sun JL, Nan Y (2008) Analysis of the critical rainfall thresholds for mudflow in Beijing, China. *Geological*
491 *Bulletin of China* 27(5): 674-680. (in Chinese)
- 492 Baum RL, Godt JW (2010). Early warning of rainfall-induced shallow landslides and debris flows in the USA.
493 *Landslides*, 7(3):259-272.
- 494 Caine, N (1980) The rainfall intensity-duration control of shallow landslides and debris flows. *Physical Geography*
495 62A (1-2):23-27
- 496 Campbell RH (1975) Debris Flow Originating from Soil Slip during Rainstorm in Southern California. *Q. Engineering*
497 *Geologist* 7: 339-349. DOI:10.1144/GSL.QJEG.1974.007.04.04
- 498 Cannon, Susan H., et al. (2008) Storm rainfall conditions for floods and debris flows from recently burned areas in
499 southwestern Colorado and southern California. *Geomorphology* 96(3): 250-269.
- 500 Chen, Su-Chin, and Bo-Tsung Huang (2010) Non-structural mitigation programs for sediment-related disasters after
501 the Chichi Earthquake in Taiwan. *Journal of Mountain Science* 7(3): 291-300.
- 502 Chen YS (2008) An influence of earthquake on the occurrence of landslide and debris flow. Taipei: National Cheng
503 Kung University.
- 504 Chen YJ, Yu B, Zhu Y, et al. (2013) Characteristics of critical rainfall of debris flow after earthquake - a case study of
505 the Xiaogangjian gully. *Journal of Mountain Science* 31(3): 356-361. (in Chinese)
- 506 Cheng ZL, Zhu PY, Liu LJ (1998) The Relationship between Debris Flow Activity and Rainfall Intensity. *Journal of*
507 *Natural Disasters* 7 (1): 118-120. (in Chinese)
- 508 Chen NS, Yang CL, Zhou W, et al. (2009) The Critical Rainfall Characteristics for Torrents and Debris Flows in the
509 Wenchuan Earthquake Stricken Area. *Journal of Mountain Science* 6: 362-372. DOI: 10.1007/s11629-009-1064-9
- 510 Cui P (1991) Experiment Research of the Initial Condition and Mechanism of Debris Flow. *Chinese Science Bulletin*
511 21:1650-1652. (in Chinese)
- 512 Cui P, Hu KH, Zhuang JQ, Yang Y, Zhang J (2011) Prediction of debris-flow danger area by combining hydro-logical
513 and inundation simulation methods. *Journal of Mountain Science* 8(1): 1-9. doi: 10.1007/s11629-011-2040-8
- 514 Dahal RK, Hasegawa S, Nonomura A, et al. (2009) Failure characteristics of rainfall-induced shallow landslides in
515 granitic terrains of Shikoku Island of Japan. *Environmental geology* 56(7): 1295-1310. DOI:
516 10.1007/s00254-008-1228-x
- 517 Degetto M, Gregoretti C, Bernard M (2015) Comparative analysis of the differences between using LiDAR
518 contour-based DEMs for hydrological modeling of runoff generating debris flows in the Dolomites. *Front. Earth Sci.*
519 3, 21. doi: 10.3389/feart.2015.00021
- 520 Gregoretti C, Degetto M, Boreggio M (2016) GIS-based cell model for simulating debris flow runoff on a fan. *Journal*



- 521 of Hydrology 534: 326-340. doi: 10.1016/j.jhydrol.2015.12.054
- 522 Guido Rianna, Luca Pagano, Gianfranco Urciuoli (2014) Rainfall patterns triggering shallow flowslides in pyroclastic
523 soils. *Engineering Geology*, 174: 22-35 doi: 10.1016/j.enggeo.2014.03.004
- 524 Guo, X.J., Cui, P., Li, Y., 2013. Debris flow warning threshold based on antecedent rainfall: a case study in Jiangjia
525 Ravine, Yunnan, China. *J. Mt. Sci.* 10 (2), 305–314.
- 526 Guzzetti, F., Peruccacci, S., Rossi, M., & Stark, C. P. (2008). The rainfall intensity–duration control of shallow
527 landslides and debris flows: an update. *Landslides*, 5(1), 3-17.
- 528 Hu M J, Wang R (2003) Testing Study of the Correlation among Landslide, Debris Flow and Rainfall in Jiangjia Gully.
529 *Chinese Journal of Rock Mechanics and Engineering*, 22(5): 824–828 (in Chinese)
- 530 Hong Y, Hiura H, Shino K, et al. (2005) The influence of intense rainfall on the activity of large-scale crystalline schist
531 landslides in Shikoku Island, Japan. *Landslides* 2(2): 97-105. DOI: 10.1007/s10346-004-0043-z
- 532 Hu W, Dong XJ, Wang GH, van Asch TWJ, Hicher PY (2016) Initiation processes for run-off generated debris flows
533 in the Wenchuan earthquake area of China. *Geomorphology* 253: 468–477. doi: 10.1016/j.geomorph.2015.10.024
- 534 Jianqi Zhuang, Peng Cui, Gonghui Wang, et al. (2015) Rainfall thresholds for the occurrence of debris flows in the
535 Jiangjia Gully, Yunnan Province, China. *Engineering Geology*, 195: 335-346.
- 536 Jibson RW (1989) Debris flows in southern Puerto Rico. *Geological Society of America Special Papers* 236: 29-56.
537 DOI: 10.1130/SPE236-p29
- 538 Jun Wang, Shun Yang, Guoqiang Ou, et al. (2017) Debris flow hazards assessment by combing numerical simulation
539 and land utilization. *Bulletin of Engineering Geology and the Environment*, 1-15. Doi: 10.1007/s10064-017-1006-7.
- 540 Liang GM, Yao LK (2008) Study on the critical rainfall for debris flows. *Lu Ji Gongcheng* 6: 3-5. (in Chinese)
- 541 Liu YH, Tang C, Li TF, et al. (2009) Statistical relations between geo-hazards and rain type. *Journal of Engineering*
542 *Geology* 17(5): 656-661. (in Chinese)
- 543 Liu JF, You Y, Chen XZ, Fan JR (2010) Identification of potential sites of debris flows in the upper Min River
544 drainage, following environmental changes caused by the Wenchuan earthquake. *Journal of Mountain Science* 3:
545 255-263. doi: 10.1007/s11629-010-2017-z
- 546 McCoy SW, Kean JW, Coe JA, Tucker GE, Staley DM, Waskiewicz WA (2012) Sediment entrainment by debris flows:
547 In situ measurements from the head waters of a steep catchment. *J. Geophys. Res.* 117, F03016. doi:
548 10.1029/2011JF002278
- 549 Mohamad Ayob Mohamadi, Ataollah Kaviani (2015) Effects of rainfall patterns on runoff and soil erosion in field plots.
550 *International Soil and Water Conservation Research* 3: 273-281.
551 <http://dx.doi.org/10.1016/j.iswcr.2015.10.001> Imaizumi F, Sidle RC, Tsuchiya S, Ohsaka O (2006)
552 Hydrogeomorphic processes in a steep debris flow initiation zone. *Geophys. Res. Lett.* 33, L10404. doi:
553 10.1029/2006GL026250
- 554 Iverson RM, Lahusen RG (1989) Dynamic Pore-Pressure Fluctuations in Rapidly Shearing Granular Materials.
555 *Science* 246 (4931): 796–799. DOI: 10.1126/science.246.4931.796
- 556 Pan HL, Ou GQ, Hang JC, et al. (2012) Study of rainfall threshold of debris flow forewarning in data lack areas. *Rock*
557 *and Soil Mechanics* 33(7): 2122-2126. (in Chinese)



- 558 Pan HL, Huang JC, Wang R, et al. (2013) Rainfall Threshold Calculation Method for Debris Flow Pre-Warning in
559 Data-Poor Areas. *Journal of Earth Science* 24(5): 854–862. DOI:10.1007/s12583-013-0377-3
- 560 Rosi A, Lagomarsino D, Rossi G, Segoni S, Battistini A, Casagli N (2015) Updating EWS rainfall thresholds for the
561 triggering of landslides. *Nature Hazard* 78:297–308
- 562 Saito H, Nakayama D, Matsuyama H (2010) Relationship between the initiation of a shallow landslide and rainfall
563 intensity–duration thresholds in Japan. *Geomorphology* 118(1): 167–175. DOI:
564 10.1016/j.geomorph.2009.12.016 Segoni S, Battistini A, Rossi G, Rosi A, Lagomarsino D, Catani F, Moretti S,
565 Casagli N (2015) Technical note: an operational landslide early warning system at regional scale based on
566 space–time variable rainfall thresholds. *Nat Hazards Earth Syst Sci* 15: 853–861
- 567 Shied CL, Chen LZ (1995) Developing the critical line of debris –flow occurrence. *Journal of Chinese Soil and Water*
568 *Conservation* 26(3):167–172. (in Chinese)
- 569 Shieh CL, Chen YS, Tsai YJ, et al (2009) Variability in rainfall threshold for debris flow after the Chi-Chi earthquake
570 in central Taiwan, China. *International Journal of Sediment Research* 24(2): 177–188.
- 571 Staley, D.M., Kean, J.W., Cannon, S.C., Schmidt, K.M., Laber, J.L. (2013) Objective definition of rainfall
572 intensity–duration thresholds for the initiation of post-fire debris flows in southern California, *Landslides* 10,
573 547–562
- 574 Takahashi T (1978) Mechanical Characteristics of Debris Flow. *Journal of the Hydraulics Division* 104:1153–1169
- 575 Tang C, Zhu J, Li WL (2009) Rainfall-triggered debris flows following the Wenchuan earthquake. *Bull Eng Geol*
576 *Environ* 68(2):187–194. DOI: 10.1007/s10064-009-0201-6
- 577 Tang C, Van Asch TWJ, Chang M, et al.(2012) Catastrophic debris flows on 13 August 2010 in the Qingping area,
578 southwestern China: the combined effects of a strong earthquake and subsequent rainstorms.
579 *Geomorphology* 139–140:559–576. DOI: 10.1016/j.geomorph.2011.12.021
- 580 Tang C, Zhu J, Chang M, et al. (2012) An empirical–statistical model for predicting debris-flow runout zones in the
581 Wenchuan earthquake area. *Quaternary International* 250:63–73. DOI:10.1016/j.quaint.2010.11.020.
- 582 Tecca PR, Genevois R (2009) Field observations of the June 30, 2001 debris flow at Acquabona (Dolomites, Italy).
583 *Landslides* 6(1): 39–45. doi: 10.1007/s10346-009-0145-8
- 584 Tian B, Wang YY, Hong Y (2008) Weighted relation between antecedent rainfall and process precipitation in debris
585 flow prediction—A case study of Jiangujia gully in Yunnan province. *Bulletin of Soil and Water Conservation* 28(2):
586 71–75. (in Chinese)
- 587 Tiranti D, Deangeli C (2015) Modeling of debris flow depositional patterns according to the catchment and sediment
588 source area characteristics. *Front. Earth Sci.* 3, 8. doi: 10.3389/feart.2015.00008
- 589 Tofani et al., Soil characterization for shallow landslides modeling: a case study in the Northern Apennines (Central
590 Italy). 2017. *Landslides* 14:755–770, DOI 10.1007/s10346-017-0809-8
- 591 Y.Zhao, F. Wei, H. Yang, et al. (2011) Discussion on Using Antecedent Precipitation Index to Supplement Relative Soil
592 Moisture Data Series. *Procedia Environment Sciences* 10: 1489–1495.
- 593 Wang EC, Meng QR (2009) Mesozoic and cenozoic tectonic evolution of the Longmenshan fault belt. *Science in China*
594 *Series D: Earth Sciences* 52(5): 579–592. DOI:10.1007/s11430-009-0053-8
- 595 Wang J, Ou GQ, Yang S, Lu GH, et al. (2013) Applicability of geomorphic information entropy in the post-earthquake



- 596 debris flow risk assessment. *Journal of Mountain Science* 31(1): 83-91. (in Chinese)
- 597 Wang J, Yu Y, Yang S, et al.(2014)A Modified Certainty Coefficient Method (M-CF) for Debris Flow Susceptibility
- 598 Assessment: A Case Study for the Wenchuan Earthquake Meizoseismal Areas. *Journal of Mountain Science*11(5):
- 599 1286-1297. DOI: 10.1007/s11629-013-2781-7
- 600 Wieczorek GF (1987) Effect of rainfall intensity and during in debris flows in central Santa Cruz Mountain. California.
- 601 *Engineering Geology* 7: 93-104. DOI: 10.1130/REG7-p93
- 602 Wilson, RC, Jayko AS (1997) Preliminary Maps ShowingRainfall Thresholds for Debris-Flow Activity, San
- 603 Franciscoby Region, California. U.S. Geological SurveyOpen-File Report 97-745 F
- 604 Winter, M. G., et al. (2010) Debris flow, rainfall and climate change in Scotland. *Quarterly Journal of Engineering*
- 605 *Geology and Hydrogeology* 43(4): 429-446.
- 606 Xu ZQ, Ji SC, Li HB, et al. (2008)Uplift of the Longmen Shan range and the Wenchuan earthquake. *Episodes* 31(3):
- 607 291-301
- 608 Xu Q, Zhang S, Li WL, et al.(2012) The 13 August 2010catastrophic debris flows after the 2008 Wenchuan earthquake,
- 609 China. *Natural hazards and earth system sciences* 12(1):201–216. DOI: 10.5194/nhess-12-201-2012
- 610 Yao LK (1988) A research on the calculation of criticalrainfall with frequency of debris flow and torrentialrain.
- 611 *Journal of Soil and Water Conservation* 2(4): 72-78 (in Chinese)
- 612 Ye SZ (1992) Hydrological calculation. Water conservancy and Hydropower Press, 111.
- 613 Zhou, W., & Tang, C. (2014). Rainfall thresholds for debris flow initiation in the Wenchuan earthquake-stricken area,
- 614 southwestern China. *Landslides*, 11(5), 877-887.
- 615 Zhuang JQ, Cui P, Ge YG, et al. (2009) Relationship between rainfall characteristics and totalamount of debris flow.
- 616 *Journal of Beijing Forestry University* 31(4): 77-83 (in Chinese)
- 617 Zhang SJ, Yang HJ, Wei FQ, et al. (2014)A Model of Debris Flow Forecast Based on the Water-SoilCoupling
- 618 Mechanism. *Journal of Earth Science*, 25(4): 757-763. DOI:10.1007/s12583-014-0463-1
- 619 Zhenlei Wei, Yuequan Shang, Yu Zhao, et al. (2017) Rainfall threshold for initiation of channelized debris flows in a
- 620 small catchment based on in-site measurement. *Engineering Geology*, 217, 23-34.